

FFI RAPPORT

POLARIMETRIC SCATTERING CALCULATIONS BASED ON MAXWELL'S EQUATIONS FOR VERY HIGH RESOLUTION SAR

ELDHUSET Knut

FFI/RAPPORT-2004/03770

**POLARIMETRIC SCATTERING CALCULATION
BASED ON MAXWELL'S EQUATIONS FOR
VERY HIGH RESOLUTION SAR**

ELDHUSET Knut

FFI/RAPPORT-2004/03770

FORSVARETS FORSKNINGSINSTITUTT
Norwegian Defence Research Establishment
P O Box 25, NO-2027 Kjeller, Norway

1) PUBL/REPORT NUMBER FFI/RAPPORT-2004/03770 1a) PROJECT REFERENCE FFI-III/839/170	2) SECURITY CLASSIFICATION UNCLASSIFIED 2a) DECLASSIFICATION/DOWNGRADING SCHEDULE -	3) NUMBER OF PAGES 33		
4) TITLE POLARIMETRIC SCATTERING CALCULATION BASED ON MAXWELL'S EQUATIONS FOR VERY HIGH RESOLUTION SAR				
5) NAMES OF AUTHOR(S) IN FULL (surname first) ELDHUSET Knut				
6) DISTRIBUTION STATEMENT Approved for public release. Distribution unlimited. (Offentlig tilgjengelig)				
7) INDEXING TERMS IN ENGLISH: <table style="width: 100%; border: none;"> <tr> <td style="width: 50%; vertical-align: top;"> a) <u>Electromagnetic waves</u> b) <u>Scattering</u> c) <u>Polarization</u> d) <u>SAR processing</u> e) <u>Satellites</u> </td> <td style="width: 50%; vertical-align: top;"> IN NORWEGIAN: a) <u>Elektromagnetiske bølger</u> b) <u>Spredning</u> c) <u>Polarisasjon</u> d) <u>SAR prosessering</u> e) <u>Satellitter</u> </td> </tr> </table>			a) <u>Electromagnetic waves</u> b) <u>Scattering</u> c) <u>Polarization</u> d) <u>SAR processing</u> e) <u>Satellites</u>	IN NORWEGIAN: a) <u>Elektromagnetiske bølger</u> b) <u>Spredning</u> c) <u>Polarisasjon</u> d) <u>SAR prosessering</u> e) <u>Satellitter</u>
a) <u>Electromagnetic waves</u> b) <u>Scattering</u> c) <u>Polarization</u> d) <u>SAR processing</u> e) <u>Satellites</u>	IN NORWEGIAN: a) <u>Elektromagnetiske bølger</u> b) <u>Spredning</u> c) <u>Polarisasjon</u> d) <u>SAR prosessering</u> e) <u>Satellitter</u>			
THESAURUS REFERENCE: 8) ABSTRACT A method for raw signal generation for extended SAR (Synthetic Aperture Radar) scenes with very high resolution is described. Such a simulator shall handle resolution better than 30 cm, squinted geometry, elliptical orbit motion and use a polarimetric reflectivity matrix. Classical polarimetric scattering theory is based on electromagnetic harmonic fields using Maxwell's equations, Green's function, Huygens' principle and Kirchhoff's approximation. Here, the scattering theory is modified for a chirp field. Calculated expressions for the scattered chirp field or the reflectivity matrix in the single scattering case are presented. Such a reflectivity matrix can then be input to the Inverse-EETF4 (Extended Exact Transfer Function 4 th order) for raw data generation.				
9) DATE 2004-11-3	AUTHORIZED BY This page only Johnny Bardal	POSITION Director		

CONTENTS

	Page
1 INTRODUCTION	7
2 DIFFERENT FORMS OF MAXWELL'S EQUATIONS	9
2.1 The Helmholtz equation	8
2.2 Propagation of a chirp field	9
2.3 Maxwell's equations and a chirp field	10
3 POLARIZATION OF UNIFORM PLANE CHIRPS	12
3.1 Linear and circular polarized chirp field	12
3.2 Elliptical polarized chirp field	14
4 GREEN'S FUNCTION	19
5 HUYGENS' PRINCIPLE	20
6 KIRCHHOFF'S APPROXIMATION	22
7 CALCULATION OF SCATTERING ELEMENTS FOR SPECIFIED GEOMETRY	27
8 INVERSE-EETF FOR RAW DATA SIMULATION	30
9 CONCLUSION	33
REFERENCES	33

POLARIMETRIC SCATTERING CALCULATION BASED ON MAXWELL'S EQUATIONS FOR VERY HIGH RESOLUTION SAR

1 INTRODUCTION

One of the objectives in HIGHSAT 839 was to build up competence in polarimetric SAR in the Norwegian defence. Initially, the intention was to start with analysis of polarimetric data from RADARSAT-2. The postponement of the launch of RADARSAT-2 data made it possible to do a study of fundamentals in polarimetric SAR. In defence a very important problem is to develop techniques for detection and identification of hard targets in SAR images. Hard targets may be man-made objects such as ships, vehicles, buildings and other infrastructure on land. It is assumed that a deeper understanding of the hard target properties will be achieved by using sound physical modelling of the scattering than using analysis of the polarimetric data alone. Signatures based on polarimetric data and electromagnetic scattering modeling must be compared in order to gain best possible insight in the reflection mechanisms from the targets which may have different kind of backgrounds. Background regions are mostly dominated by clutter in SAR images. Another aspect in the modeling of signatures in SAR images is the SAR imaging mechanism. To do complete modeling, the generation of SAR raw data must be done by an inverse SAR processing algorithm.

In the near future, space borne SAR with resolution better than 1 m will be available. This is a challenge for scattering modelling as well as SAR processing of the raw data. Azimuth and range signals with extremely high bandwidths have to be handled carefully. In scattering theory, time harmonic signals are usually assumed. For very high resolution systems, however, the chirp bandwidth compared to the carrier frequency is considerable. The large bandwidth of the range signal makes it necessary to modify existing expressions in scattering theory. This modification of the scattering theory in this report is new. The approximation of the azimuth signal in the SAR processor is also a critical point, especially with some squint.

In Chapter 2 we review Maxwell's equations and consider plane chirp fields. The usual treatment of Maxwell's equations in the literature considers harmonic fields. In Section 2.1 we review the Helmholtz equation and in Section 2.2 we show that a chirp field satisfies this equation. In Section 2.3 we consider Maxwell's equation and a chirp field and show that a set of harmonic fields has to be used for scattering calculations. In Chapter 3 we analyse properties of uniform plane chirps. The linear and circular polarized chirp fields are discussed in Section 3.1 and the elliptical polarized field in Section 3.2. In Chapters 4 and 5 the Green's function and Huygens' principle are reviewed and extended for chirp fields using a set of harmonic fields. In Section 7 the Kirchhoff's approximation is used to express the scattered field in the single scattering case. The expression for the local reflected field in the specular direction is modification compared to the literature. The scattering elements are calculated for simple geometry in Section 7. Finally, in Section 8 we show how the reflectivity matrix can be

input in the Inverse-EETF4 algorithm to generate raw data. The reflectivity matrix can be calculated from the expression for the scattered field.

2 DIFFERENT FORMS OF MAXWELL'S EQUATIONS

If we assume that the net free charge is zero, the Maxwell's equations in point form can be written (Paul and Nasar (1987))

$$\nabla \times \vec{E}(\vec{r}, t) = -\mu \frac{\partial \vec{H}(\vec{r}, t)}{\partial t} \quad (2.1)$$

$$\nabla \times \vec{H}(\vec{r}, t) = \sigma \vec{E}(\vec{r}, t) + \varepsilon \frac{\partial \vec{E}(\vec{r}, t)}{\partial t} \quad (2.2)$$

$$\nabla \cdot \vec{H}(\vec{r}, t) = 0 \quad (2.3)$$

$$\nabla \cdot \vec{E}(\vec{r}, t) = 0 \quad (2.4)$$

where Eq. (2.1) is the Faraday law and Eq. (2.2) is the Ampere law. ε and μ are the permittivity and permeability. For free space the conductivity $\sigma = 0$. $\vec{E}(\vec{r}, t)$ is the space and time dependent electric field and $\vec{H}(\vec{r}, t)$ is the magnetic field.

2.1 The Helmholtz equation

The calculations in this section follow Paul and Nasar (1987), p. 278. Taking the curl of Eq. (2.1) we obtain

$$\begin{aligned} \nabla \times \nabla \times \vec{E}(\vec{r}, t) &= -\mu \left(\nabla \times \frac{\partial \vec{H}(\vec{r}, t)}{\partial t} \right) = -\mu \frac{\partial}{\partial t} \left(\nabla \times \vec{H}(\vec{r}, t) \right) = \\ &= -\mu \frac{\partial}{\partial t} \left(\sigma \vec{E}(\vec{r}, t) + \varepsilon \frac{\partial \vec{E}(\vec{r}, t)}{\partial t} \right) \end{aligned}$$

which can be rewritten as

$$\nabla \times \nabla \times \vec{E}(\vec{r}, t) = -\mu\sigma \frac{\partial \vec{E}(\vec{r}, t)}{\partial t} - \mu\varepsilon \frac{\partial^2 \vec{E}(\vec{r}, t)}{\partial t^2} \quad (2.5)$$

In the same way we take the curl of Eq. (2.2) and we find

$$\nabla \times \nabla \times \vec{H}(\vec{r}, t) = -\mu\sigma \frac{\partial \vec{H}(\vec{r}, t)}{\partial t} - \mu\epsilon \frac{\partial^2 \vec{H}(\vec{r}, t)}{\partial t^2} \quad (2.6)$$

We now use a well known vector identity

$$\nabla \times \nabla \times \vec{A} = \nabla(\nabla \cdot \vec{A}) - \nabla^2 \vec{A} \quad (2.7)$$

and Eqs. (2.3) and (2.4). Using Eq. (2.5) we get

$$\nabla \times \nabla \times \vec{E}(\vec{r}, t) = \nabla(\nabla \cdot \vec{E}(\vec{r}, t)) - \nabla^2 \vec{E}(\vec{r}, t) = -\nabla^2 \vec{E}(\vec{r}, t) = -\mu\sigma \frac{\partial \vec{E}(\vec{r}, t)}{\partial t} - \mu\epsilon \frac{\partial^2 \vec{E}(\vec{r}, t)}{\partial t^2}$$

from which we see that

$$\nabla^2 \vec{E}(\vec{r}, t) = \mu\sigma \frac{\partial \vec{E}(\vec{r}, t)}{\partial t} + \mu\epsilon \frac{\partial^2 \vec{E}(\vec{r}, t)}{\partial t^2} \quad (2.8)$$

$$\nabla^2 \vec{H}(\vec{r}, t) = \mu\sigma \frac{\partial \vec{H}(\vec{r}, t)}{\partial t} + \mu\epsilon \frac{\partial^2 \vec{H}(\vec{r}, t)}{\partial t^2} \quad (2.9)$$

which are called the Helmholtz equations. These two vector equations consist of 6 scalar equations. Taking the x-component of the first one as an example,

$$\nabla^2 E_x(\vec{r}, t) = \mu\sigma \frac{\partial E_x(\vec{r}, t)}{\partial t} + \mu\epsilon \frac{\partial^2 E_x(\vec{r}, t)}{\partial t^2} \quad (2.10)$$

where

$$\nabla^2 E_x(\vec{r}, t) = \frac{\partial^2 E_x(\vec{r}, t)}{\partial x^2} + \frac{\partial^2 E_x(\vec{r}, t)}{\partial y^2} + \frac{\partial^2 E_x(\vec{r}, t)}{\partial z^2}$$

2.2 Propagation of a chirp field

It is known that harmonic fields satisfy Maxwell equations, which is shown for a harmonic wave in Example 5.4 p. 236 in Paul and Nasar (1987). In SAR systems the radar waves are not harmonic waves, however, they are chirps. Here we show that a chirp field satisfies Maxwell's equations by using the Helmholtz equation. For simplicity we assume that a plane chirp field has only an x-component which propagates in the z direction. Let the x-component of the chirp field be

$$E_x(z, t) = E_0 \sin \left[\omega \left(t - \frac{z}{c} \right) + \frac{1}{2} K \left(t - \frac{z}{c} \right)^2 \right] \quad (2.11)$$

where ω is the angular carrier frequency and K is the chirp rate. Since we assume that the y and z components of the field, $E_y(z, t)$ and $E_z(z, t)$, are zero and we assume free space, $\sigma = 0$, the Helmholtz equation in Eq.(2.10) becomes

$$\frac{\partial^2 E_x(z, t)}{\partial z^2} = \mu_0 \epsilon_0 \frac{\partial^2 E_x(z, t)}{\partial t^2} \quad (2.12)$$

Calculation of the left side of Eq. (2.12) yields

$$\begin{aligned} \frac{\partial^2 E_x}{\partial z^2} = E_0 \left(\frac{1}{c} \right) & \left\{ \left[\frac{2K}{c} \cos \left[\omega \left(t - \frac{z}{c} \right) + K \left(t - \frac{z}{c} \right)^2 \right] \right] - \left[\omega + 2K \left(t - \frac{z}{c} \right) \right]^2 - \right. \\ & \left. \left[\omega + 2K \left(t - \frac{z}{c} \right) \right]^2 \sin \left[\omega \left(t - \frac{z}{c} \right) + K \left(t - \frac{z}{c} \right)^2 \right] \right\} \end{aligned} \quad (2.13)$$

Calculation of the right side is similar as for Eq. (2.13) and it can be seen that

$$\frac{\partial^2 E_x(z, t)}{\partial z^2} = \frac{1}{c^2} \frac{\partial^2 E_x(z, t)}{\partial t^2} \quad (2.14)$$

We compare Eqs.(2.12) and (2.14) and see that they are identical if the speed of light is equal to the inverse square of the product of the free space permittivity and permeability $c = 1/\sqrt{\mu_0 \epsilon_0}$. In particular Eq. (2.14) is satisfied for $K = 0$, which is a harmonic wave.

2.3 Maxwell's equations and a chirp field

For a harmonic field the time dependent parts can be totally separated from the space dependent parts. If the bandwidth of a chirp field is sufficiently small we can also make that assumption in an approximate manner. For a harmonic field we have the electric field

$$\vec{E}(x, y, z, t) = \vec{E}(x, y, z) \cdot \exp(j\omega t) \quad (2.15)$$

and the magnetic field

$$\vec{H}(x, y, z, t) = \vec{H}(x, y, z) \cdot \exp(j\omega t) \quad (2.16)$$

If we put Eq. (2.15) into the Faraday law in Eq. (2.1) we get

$$\nabla \times \vec{E}(x, y, z) = -j\omega \mu \vec{H}(x, y, z) \quad (2.17)$$

Eq. (2.17) can be found in Paul and Nasar (1987) or in Kong (1986). We see from Eq. (2.11) that a harmonic field ($K = 0$) can be separated in a time dependent part and a space dependent part. This is not the case for the chirp field ($K \neq 0$) due to the cross coupling of space and time

variables. Now, if for sufficiently small chirp bandwidth we assume for a chirp field that the time dependency is approximately separated from the the space dependency the electric field can be written

$$\vec{E}(x, y, z, t) \approx \vec{E}(x, y, z) \cdot \exp\left[j\left(\omega t + \frac{1}{2} K t^2\right)\right] \quad (2.18)$$

and the magnetic field

$$\vec{H}(x, y, z, t) \approx \vec{H}(x, y, z) \cdot \exp\left[j\left(\omega t + \frac{1}{2} K t^2\right)\right] \quad (2.19)$$

Taking the time derivative of Eq. (2.19) we get

$$\frac{\partial \vec{H}(x, y, z, t)}{\partial t} \approx \vec{H}(x, y, z) j(\omega + Kt) \exp\left[j\left(\omega t + \frac{1}{2} K t^2\right)\right]$$

The Faraday law can then be approximated for a chirp field

$$\nabla \times \vec{E}(x, y, z) \approx -j(\omega + Kt) \mu \vec{H}(x, y, z) \quad (2.20)$$

which shows that we cannot get an equation that is only space dependent as in the harmonic case. If we consider a chirp field with a set of harmonic fields where the frequency of harmonic field number n is

$$\omega_n = \omega + Kt_n \quad (2.21)$$

we have a set of Faraday equations, one equation for each of the harmonic fields

$$\nabla \times \vec{E}_n(x, y, z) = -j\omega_n \mu \vec{H}_n(x, y, z) \quad (2.22)$$

In the same way we find that the Ampere law can be written in an approximate form for a chirp field

$$\frac{\partial \vec{E}(x, y, z, t)}{\partial t} \approx \vec{E}(x, y, z) j(\omega + Kt) \exp\left[j\left(\omega t + \frac{1}{2} K t^2\right)\right]$$

Then the Ampere law can be approximated for a chirp field

$$\nabla \times \vec{H}(x, y, z) \approx \vec{J}(x, y, z) + j(\omega + Kt) \epsilon \vec{E}(x, y, z) \quad (2.23)$$

where the current density is defined as $\vec{J} = \sigma \vec{E}$ in Paul and Nasar (1987), p. 234. For each of the short harmonic fields we get

$$\nabla \times \vec{H}_n(x, y, z) = \vec{J}_n(x, y, z) + j\omega_n \varepsilon \vec{E}_n(x, y, z) \quad (2.24)$$

We underline that treatment of the chirp field as a set of harmonic fields is an approximation. The number of harmonic fields must be chosen as a function of the chirp bandwidth.

3 POLARIZATION OF UNIFORM PLANE CHIRPS

3.1 Linear and circular polarized chirp field

We have shown that a chirp field satisfies Maxwell's equations. Here we consider different states of polarimetric fields as in Section 6.5 in Paul and Nasar (1987), however, we use an electric chirp field vector instead of a harmonic field vector. This introduces new properties of the fields. Here we define an electric chirp field vector with horizontal polarization as

$$\vec{E}(x, y, z, t) = E_0 \sin \left[\omega \left(t - \frac{z}{c} \right) + \frac{1}{2} K \left(t - \frac{z}{c} \right)^2 \right] \cdot \vec{a}_x \quad (3.1)$$

which propagates in the z direction and the electric field vector points in the x direction in a Cartesian coordinate system. \vec{a}_x can for example be the *horizontal polarization* direction of a wave and \vec{a}_y can be the *vertical polarization* direction. The magnetic chirp field vector is defined

$$\vec{H}(x, y, z, t) = \frac{E_0}{\eta} \sin \left[\omega \left(t - \frac{z}{c} \right) + \frac{1}{2} K \left(t - \frac{z}{c} \right)^2 \right] \cdot \vec{a}_y \quad (3.2)$$

which is perpendicular to the electric field and $\eta = \sqrt{\mu/\varepsilon}$ is the intrinsic impedance. If we now consider the sum of a horizontal polarized wave with amplitude E_{m1} and a vertical polarized wave with amplitude E_{m2} and an additional phase θ we get

$$\begin{aligned} \vec{E}(x, y, z, t) = & E_{m1} \sin \left[\omega \left(t - \frac{z}{c} \right) + \frac{1}{2} K \left(t - \frac{z}{c} \right)^2 \right] \cdot \vec{a}_x + \\ & E_{m2} \sin \left[\omega \left(t - \frac{z}{c} \right) + \frac{1}{2} K \left(t - \frac{z}{c} \right)^2 + \theta \right] \cdot \vec{a}_y \end{aligned} \quad (3.3)$$

which propagates in the z direction. We consider some polarization states of this chirp field.

CASE 1: Linear polarization

If we choose

$$E_{m1} = E_{m2}, \theta = 0 \quad (3.4)$$

and $z = 0$ we get

$$\vec{E}\Big|_{z=0} = E_{m1} \sin\left[\omega t + \frac{1}{2} K t^2\right] \cdot (\vec{a}_x + \vec{a}_y) \quad (3.5)$$

This is an electric field vector with direction 45° relative to the x-axis and changes its length with rate $\omega + Kt$. In the harmonic case the rate is ω and constant as function of the time.

CASE 2: Linear polarization

If we let the amplitudes of the horizontal and vertical polarization be different and the phase angle zero we have

$$E_{m1} \neq E_{m2}, \theta = 0 \quad (3.6)$$

and

$$\vec{E}\Big|_{z=0} = E_{m1} \cos\left[\omega t + \frac{1}{2} K t^2\right] \cdot \left(\vec{a}_x + \frac{E_{m2}}{E_{m1}} \vec{a}_y\right) \quad (3.7)$$

In this case the electric field vector oscillates in a direction $\tan^{-1}(E_{m2}/E_{m1})$ relative to the x-axis and changes its length with rate $\omega + Kt$. In the harmonic case the length of the electric field vector length changes with a constant rate ω .

CASE 3: Circular polarization

If we let the amplitudes of the horizontal and vertical polarization be equal and the phase angle between the two states is -90° we have

$$E_{m1} = E_{m2}, \theta = -90^\circ \quad (3.8)$$

$$\begin{aligned} \vec{E}\Big|_{z=0} &= E_{m1} \left\{ \cos\left[\omega t + \frac{1}{2} K t^2\right] \cdot \vec{a}_x + \cos\left[\omega t + \frac{1}{2} K t^2 - 90^\circ\right] \cdot \vec{a}_y \right\} = \\ &E_{m1} \left\{ \cos\left[\omega t + \frac{1}{2} K t^2\right] \cdot \vec{a}_x + \sin\left[\omega t + \frac{1}{2} K t^2\right] \cdot \vec{a}_y \right\} \end{aligned} \quad (3.9)$$

The length of this field vector is E_{m1} at all times. For harmonic waves, when $K = 0$ the electric field vector rotates with constant angular speed ω , and for a chirp when $K \neq 0$, the electric field vector rotates with the tip along a circle with angular speed $\omega + Kt$, which means that the vector has a rotational acceleration.

The analysis of the magnetic field vector is the same as for the electric field and is omitted here.

3.2 Elliptical polarized chirp field

This section reviews Section 1.4 in Kong (1986) in the case of a harmonic field, however, we extend the analysis with a chirp field. We now forget the spatial variation as above ($z = 0$) of the chirp and let the horizontal polarization unit vector be $\hat{e}_h = \vec{a}_x$ and the vertical polarization unit vector be $\hat{e}_v = \vec{a}_y$. These two components are perpendicular to the direction of propagation, \hat{k} , which can be chosen along the z-axis. Then the electric field vector can be written as in Kong (1986)

$$\vec{E}(t) = E_h \hat{e}_h + E_v \hat{e}_v \quad (3.10)$$

We have a horizontal and vertical chirp component with phases ψ_v and ψ_h

$$E_h = e_h \cos\left(\omega t + \frac{1}{2} K t^2 - \psi_h\right) \quad (3.11)$$

$$E_v = e_v \cos\left(\omega t + \frac{1}{2} K t^2 - \psi_v\right) \quad (3.12)$$

Then we multiply Eq. (3.11) by $\frac{\sin \psi_v}{e_h}$ and Eq. (3.12) by $\frac{\sin \psi_h}{e_v}$ and subtract

$$\begin{aligned} \frac{E_h}{e_h} \sin \psi_v - \frac{E_v}{e_v} \sin \psi_h &= \cos\left(\omega t + \frac{1}{2} K t^2 - \psi_h\right) \cdot \sin \psi_v - \cos\left(\omega t + \frac{1}{2} K t^2 - \psi_v\right) \cdot \sin \psi_h = \\ &= \cos\left(\omega t + \frac{1}{2} K t^2\right) \cdot \sin \psi \end{aligned} \quad (3.13)$$

where

$$\psi = \psi_v - \psi_h \quad (3.14)$$

In the same manner we get

$$\frac{E_h}{e_h} \cos \psi_v - \frac{E_v}{e_v} \cos \psi_h = -\sin\left(\omega t + \frac{1}{2} K t^2\right) \cdot \sin \psi \quad (3.15)$$

We now use the fact that

$$\cos^2\left(\omega t + \frac{1}{2} K t^2\right) + \sin^2\left(\omega t + \frac{1}{2} K t^2\right) = 1 \quad (3.16)$$

Together with Eqs. 3.13 and 3.14. Then we get the equation for the polarization ellipse

$$\left(\frac{E_h}{e_h}\right)^2 + \left(\frac{E_v}{e_v}\right)^2 - 2\frac{E_h E_v}{e_h e_v} \cos \psi = \sin^2 \psi \quad (3.17)$$

The polarization ellipse is plotted in Figure 3.1 and is rotated an angle α with the E_h axis

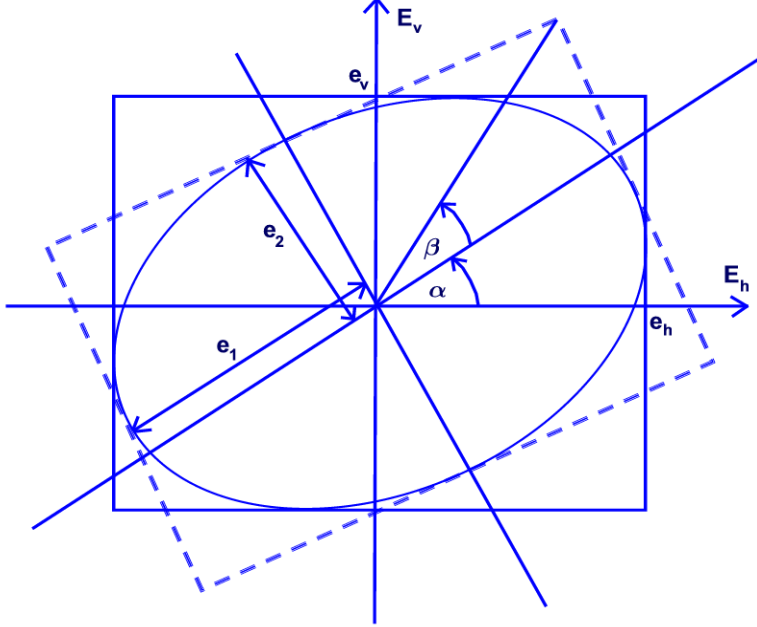


Figure 3.1 Polarization ellipse (Kong (1986) p. 20)

This means that the tip of the vector in Eq. 3.10 traces out an ellipse with an angular speed which is different for a harmonic and a chirp field. In the special case of a circle the angular speed is ω for harmonic field and ωt for a chirp as for Eq. 3.9. Now the electric field components can be expressed in terms of the horizontal and vertical components

$$\begin{pmatrix} E_1 \\ E_2 \end{pmatrix} = \begin{pmatrix} \cos \alpha & \sin \alpha \\ -\sin \alpha & \cos \alpha \end{pmatrix} \begin{pmatrix} E_h \\ E_v \end{pmatrix} \quad (3.18)$$

If we use Eq. (3.18), Eqs. 3.11 and 3.12 we get

$$\begin{aligned} e_1 \cos\left(\omega t + \frac{1}{2} K t^2 - \psi_0\right) &= e_h \cos\left(\omega t + \frac{1}{2} K t^2 - \psi_h\right) \cdot \cos \alpha + \\ e_v \cos\left(\omega t + \frac{1}{2} K t^2 - \psi_v\right) &\cdot \sin \alpha \end{aligned} \quad (3.19)$$

$$\begin{aligned}
e_2 \cos\left(\omega t + \frac{1}{2} K t^2 - \psi_0\right) &= -e_h \cos\left(\omega t + \frac{1}{2} K t^2 - \psi_h\right) \cdot \sin \alpha + \\
e_v \cos\left(\omega t + \frac{1}{2} K t^2 - \psi_v\right) \cdot \cos \alpha
\end{aligned} \tag{3.20}$$

From Eq. 3.19 we get

$$\begin{aligned}
e_1 \left[\cos\left(\omega t + \frac{1}{2} K t^2\right) \cdot \cos \psi_0 + \sin\left(\omega t + \frac{1}{2} K t^2\right) \cdot \sin \psi_0 \right] &= \\
e_h \left[\cos\left(\omega t + \frac{1}{2} K t^2\right) \cdot \cos \psi_h + \sin\left(\omega t + \frac{1}{2} K t^2\right) \cdot \sin \psi_h \right] \cdot \cos \alpha & \\
e_v \left[\cos\left(\omega t + \frac{1}{2} K t^2\right) \cdot \cos \psi_v + \sin\left(\omega t + \frac{1}{2} K t^2\right) \cdot \sin \psi_v \right] \cdot \sin \alpha &
\end{aligned} \tag{3.21}$$

and from 3.20 we get

$$\begin{aligned}
e_2 \left[\cos\left(\omega t + \frac{1}{2} K t^2\right) \cdot \cos \psi_0 + \sin\left(\omega t + \frac{1}{2} K t^2\right) \cdot \sin \psi_0 \right] &= \\
e_h \left[\cos\left(\omega t + \frac{1}{2} K t^2\right) \cdot \cos \psi_h + \sin\left(\omega t + \frac{1}{2} K t^2\right) \cdot \sin \psi_h \right] \cdot \sin \alpha & \\
e_v \left[\cos\left(\omega t + \frac{1}{2} K t^2\right) \cdot \cos \psi_v + \sin\left(\omega t + \frac{1}{2} K t^2\right) \cdot \sin \psi_v \right] \cdot \cos \alpha &
\end{aligned} \tag{3.22}$$

We see now from Eqs. (3.21) and (3.22) that we can eliminate the time dependency both for a harmonic field ($K = 0$) and a chirp field ($K \neq 0$) using Eq. 3.21 which yields two equations

$$e_1 \cos \psi_0 = e_h \cos \psi_h \cos \alpha + e_v \cos \psi_v \sin \alpha \tag{3.23}$$

$$e_1 \sin \psi_0 = e_h \sin \psi_h \cos \alpha + e_v \sin \psi_v \sin \alpha \tag{3.24}$$

In the same way we get from Eq. 3.22

$$e_1 \tan \beta \cos \psi_0 = -e_h \sin \psi_h \sin \alpha + e_v \cos \psi_v \cos \alpha \tag{3.25}$$

$$e_1 \tan \beta \sin \psi_0 = -e_h \cos \psi_h \sin \alpha - e_v \cos \psi_v \cos \alpha \tag{3.26}$$

where

$$\tan \beta = \pm \frac{e_2}{e_1} \tag{3.27}$$

Then we eliminate ψ_0 by taking the squared sums of Eqs. 3.23 and 3.24

$$\begin{aligned} e_1^2 \cos^2 \alpha + e_1^2 \sin^2 \alpha &= e_1^2 = \\ e_h^2 \cos^2 \alpha + e_v^2 \sin^2 \alpha + e_h e_v \sin 2\alpha \cos \psi \end{aligned} \quad (3.28)$$

Similarly we take the squared sums of Eqs 3.25 and 3.26 and get

$$\begin{aligned} e_1^2 \tan^2 \beta + e_1^2 \sin^2 \alpha &= e_2^2 = \\ e_h^2 \sin^2 \alpha + e_v^2 \cos^2 \alpha - e_h e_v \sin 2\alpha \cos \psi \end{aligned} \quad (3.29)$$

We see that the sum of Eqs. 3.28 and 3.29 yields

$$e_1^2 + e_2^2 = e_h^2 + e_v^2 \quad (3.30)$$

Multiplication of Eq. 3.23 by 3.25 and subtract from 3.24 multiplied by 3.26 yields

$$e_1^2 \tan \beta = e_h e_v \sin \psi \quad (3.31)$$

If we multiply 3.23 by 3.26 and subtract from 3.24 multiplied by 3.25 we get

$$2e_h e_v \cos \psi = (e_h^2 - e_v^2) \tan 2\alpha \quad (3.32)$$

We now define the four Stokes parameters

$$I = \frac{1}{\eta} (e_h^2 + e_v^2) \quad (3.33)$$

$$Q = \frac{1}{\eta} (e_h^2 - e_v^2) \quad (3.34)$$

$$U = \frac{2}{\eta} e_h e_v \cos \psi \quad (3.35)$$

$$V = \frac{2}{\eta} e_h e_v \sin \psi \quad (3.36)$$

Then we add Eqs. 3.28 and 3.29 and get

$$e_1^2 + e_1^2 \tan^2 \beta = e_h^2 + e_v^2 \quad (3.37)$$

If we use Eq. 3.33 in Eq. 3.37 we get

$$e_1^2 = \eta I \cos^2 \beta \quad (3.38)$$

If we subtract Eq. 3.29 from Eq. 3.28 and use Eqs. 3.32 and 3.38 we get

$$\eta I \cos^2 \beta (1 - \tan^2 \beta) = (e_h^2 - e_v^2) (\cos 2\alpha + \tan 2\alpha \sin 2\alpha) \quad (3.39)$$

From Eq. 3.39 and 3.34 we find

$$Q = \frac{e_h^2 - e_v^2}{\eta} = I \cos 2\beta \cos 2\alpha \quad (3.40)$$

From Eqs. 3.35, 3.32 and 3.40 we find

$$U = I \sin 2\alpha \cos 2\beta \quad (3.41)$$

And finally from Eqs. 3.36, 3.31 and 3.38 we find

$$V = I \sin 2\beta \quad (3.42)$$

We also notice that

$$I^2 = Q^2 + U^2 + V^2 \quad (3.43)$$

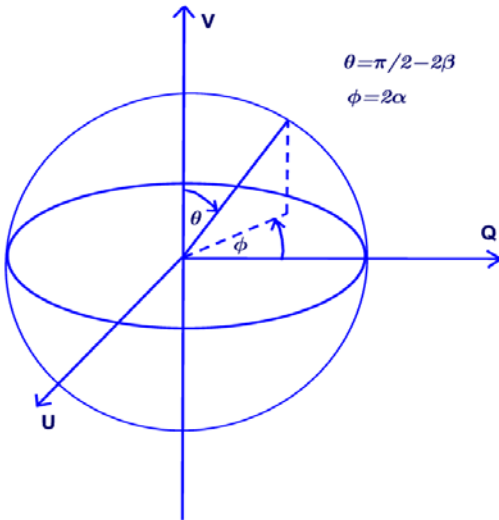


Figure 3.2 The Poincaré sphere (Kong (1986) p. 22)

Eqs. 3.40, 3.41 and 3.42 define the *Poincaré sphere* shown in Figure 3.2, which can be used to describe the polarization state of an electromagnetic wave. We see from Eqs. 3.40, 3.41 and

3.42 that the Poincaré sphere representation of the polarization states does not show any time dependency as does the polarization ellipse in Figure 3.1. This means that the Poincaré sphere does not distinguish between a harmonic wave and a chirp. It was shown in Touzi and Raney (2004) that the precision of Poincaré angle determination for ship targets is dependent on the Doppler parameter accuracies in the SAR processor. This means that characterization of moving targets (e.g. ships) will deteriorate if they are not re-focused.

4 GREEN'S FUNCTION

This chapter is a summary of Section 4.2 in Kong (1986) extended with the index n for harmonic field number. If we take the curl of Eq. (2.22) and use Eq. (2.24) we get

$$\nabla \times \nabla \times E_n(\vec{r}) - k_n^2 \vec{E}_n(\vec{r}) = j\omega_n \mu \vec{J}_n(\vec{r}) \quad (4.1)$$

where the wave number is given by

$$k_n^2 = \omega_n^2 \mu \epsilon \quad (4.2)$$

Let $G_n(\vec{r}, \vec{r}')$ be the dyadic Green's function for harmonic field number n which is the response of a point source, then the electromagnetic field can be written

$$\vec{E}_n(\vec{r}) = j\omega_n \iiint \overline{\overline{G}}_n(\vec{r}, \vec{r}') \cdot \vec{J}_n(\vec{r}') dV' \quad (4.3)$$

Let $\overline{\overline{I}}$ be the dyadic unit matrix, then the current field can be written

$$\vec{J}_n(\vec{r}) = \iiint \delta(\vec{r} - \vec{r}') \cdot \overline{\overline{I}} \cdot \vec{J}_n(\vec{r}') dV' \quad (4.4)$$

Substitution of Eq. (4.3) and (4.2) into Eq. (4.1) we get

$$\nabla \times \nabla \times \overline{\overline{G}}_n(\vec{r}, \vec{r}') - k_n^2 \overline{\overline{G}}_n(\vec{r}, \vec{r}') = \overline{\overline{I}} \delta(\vec{r} - \vec{r}') \quad (4.5)$$

The dyadic Green's function can be expressed with the scalar Green's function

$$\overline{\overline{G}}_n(\vec{r}, \vec{r}') = \left[\overline{\overline{I}} + \frac{1}{k_n^2} \nabla \nabla \right] g_n(\vec{r}, \vec{r}') \quad (4.6)$$

where the scalar function is

$$g_n(\vec{r}, \vec{r}') = \frac{\exp jk_n |\vec{r} - \vec{r}'|}{4\pi |\vec{r} - \vec{r}'|} \quad (4.7)$$

If we insert Eq. (4.6) into Eq. (4.3) and sum over N harmonic fields we get an approximation for a scattered chirp

$$\vec{E}(\vec{r}) = \sum_{n=1}^N \left\{ j\omega_n \mu \left[\bar{I} + \frac{1}{k_n^2} \nabla \nabla \right] \iiint \frac{\exp jk_n |\vec{r} - \vec{r}'|}{4\pi |\vec{r} - \vec{r}'|} J_n(\vec{r}') dV' \right\} \quad (4.8)$$

5 HUYGENS' PRINCIPLE

We review Section 5.3 in Kong (1985) extended for a chirp field with N harmonic fields. Huygens' principle states that the field solution in a region V' is completely determined by the tangential fields specified over the surface S' enclosing V' as shown in Figure 5.1. Mathematically, Huygens' principle expresses fields at an observation point \vec{r} in terms of fields at the boundary surface.

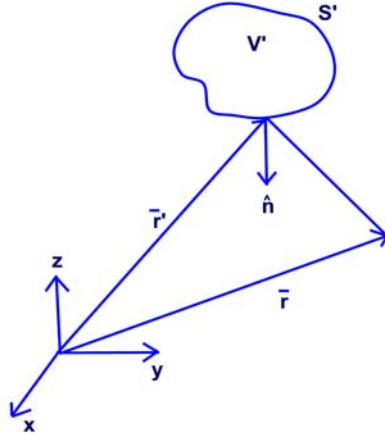


Figure 5.1 Volume V' radiates electromagnetic waves which are observed at a point \vec{r} (Fig. 5.3.1 in Kong (1986)).

To express Huygens' principle mathematically we will need the well known vector identity

$$\vec{A} \cdot (\vec{B} \times \vec{C}) = \vec{B} \cdot (\vec{C} \times \vec{A}) = -\vec{C} \cdot (\vec{A} \times \vec{B}) \quad (5.1)$$

If we use Eq. (5.1) we can write

$$\begin{aligned} & \vec{E} \cdot \left[\nabla \times \nabla \times (\bar{G} \cdot \vec{a}) \right] - \left[\nabla \times \nabla \times \vec{E} \right] \cdot (\bar{G} \cdot \vec{a}) = \\ & -\nabla \cdot \left(\vec{E} \times \nabla \times (\bar{G} \cdot \vec{a}) \right) - \nabla \cdot (\nabla \times \vec{E}) \cdot (\bar{G} \cdot \vec{a}) = \\ & -\nabla \cdot \left[\vec{E} \times \nabla \times (\bar{G} \cdot \vec{a}) + (\nabla \times \vec{E}) \times (\bar{G} \cdot \vec{a}) \right] \end{aligned} \quad (5.2)$$

where \vec{a} is an arbitrary constant vector. We also remember Gauss' theorem

$$\iiint (\nabla \cdot \vec{F}) dV' = \iint (\vec{F} \cdot \vec{n}) dS' \quad (5.3)$$

where \vec{n} is the surface normal. Now, taking a look at Eq. (5.2) we can define

$$\vec{F} = \vec{E} \times \nabla \times (\vec{G} \cdot \vec{a}) + (\nabla \times \vec{E}) \times (\vec{G} \cdot \vec{a}) \quad (5.4)$$

and let

$$\nabla \cdot \vec{F} = \vec{E} \cdot (\nabla \times \nabla \times \vec{G} \cdot \vec{a}) - (\nabla \times \nabla \times \vec{E}) \cdot (\vec{G} \cdot \vec{a}) \quad (5.5)$$

Using Eqs. (5.2), (5.3), (5.4) and (5.5) and insert the index n we find

$$\begin{aligned} & \iiint \left[\vec{E}_n(\vec{r}') \cdot \nabla \times \nabla \times \vec{G}_n(\vec{r}, \vec{r}') \cdot \vec{a} - (\nabla \times \nabla \times \vec{E}_n(\vec{r}')) \cdot \vec{G}_n(\vec{r}, \vec{r}') \cdot \vec{a} \right] dV' = \\ & \iint \left[\vec{n} \cdot (\nabla \times \vec{E}_n(\vec{r}')) \times \vec{G}_n(\vec{r}, \vec{r}') \cdot \vec{a} + \vec{n} \cdot \vec{E}_n(\vec{r}') \times \nabla \times \vec{G}_n(\vec{r}, \vec{r}') \cdot \vec{a} \right] dS' \end{aligned} \quad (5.6)$$

Now, we remember Eqs. (4.1) and (4.5). If we insert these equations into Eq. (5.6) and assume no charges in region V' , $\vec{J}(\vec{r}') = 0$, the left side of Eq. (5.6) becomes

$$\begin{aligned} & \iiint \vec{E}_n(\vec{r}') \cdot \left[\left(k_n^2 \vec{G}_n(\vec{r}, \vec{r}') + \vec{I} \delta(\vec{r} - \vec{r}') \right) - k_n^2 \vec{E}_n(\vec{r}') \vec{G}_n(\vec{r}, \vec{r}') \cdot \vec{a} \right] dV' = \\ & \iiint \left(\vec{E}_n(\vec{r}') \cdot \vec{I} \delta(\vec{r} - \vec{r}') \cdot \vec{a} \right) dV' = \vec{E}_n(\vec{r}) \vec{a} \end{aligned} \quad (5.7)$$

If we have in mind Eq. (2.17), then the right side of Eq. (5.7) and the right side of Eq. (5.6) become

$$\vec{E}_n(\vec{r}) = - \iint \left[j \omega_n \mu \vec{G}_n(\vec{r}, \vec{r}') \cdot (\vec{s} \times H_n(\vec{r}')) + \nabla \times \vec{G}_n(\vec{r}, \vec{r}') \cdot (\vec{s} \times \vec{E}_n(\vec{r}')) \right] dS' \quad (5.8)$$

We now use the expression for the dyadic Green's function in Eqs. (4.6) and (4.7) and assume that we have an observation point far away from the scattering region, that is we use the far field approximation

$$k_n |\vec{r} - \vec{r}'| \approx k_n r - k_n \hat{k}_s \cdot \vec{r}' = k_n r - \vec{k}_{n,s} \cdot \vec{r}' \quad (5.9)$$

where $\vec{k}_{n,s}$ is the scattered wave vector with wave number k_n and \hat{k}_s is the unit direction vector of the scattered field

$$k_n^2 = \left| \vec{k}_{n,s} \right|^2 = \omega_n^2 \mu_0 \epsilon_0 \quad (5.10)$$

Then the approximated Green's function for a harmonic field with wave number k_n can be written

$$\bar{\bar{G}}_n(\vec{r}, \vec{r}') \approx \left[\bar{I} + \frac{1}{k_n^2} \nabla \nabla \right] \frac{\exp(jk_n r)}{4\pi r} \exp(-j\vec{k}_{n,s} \cdot \vec{r}') \quad (5.11)$$

Calculation of Eq. (5.11) yields another expression for the Green's function in the far field

$$\bar{\bar{G}}_n(\vec{r}, \vec{r}') \approx \left[\bar{I} - \hat{k}_s \hat{k}_s \right] \frac{\exp(jk_n r)}{4\pi r} \exp(-j\vec{k}_{n,s} \cdot \vec{r}') \quad (5.12)$$

Inserting Eq. (5.12) into Eq. (5.8) yields

$$\begin{aligned} \vec{E}_s(\vec{r}) &= \sum_{n=1}^N \frac{jk_n \exp(jk_n r)}{4\pi r} \left(\bar{I} - \hat{k}_s \hat{k}_s \right) \\ &\iint \left\{ \hat{k}_s \times \left[\hat{n} \times \vec{E}_n(\vec{r}') \right] + \eta \left[\hat{n} \times \vec{H}_n(\vec{r}') \right] \right\} \exp(-j\vec{k}_{n,s} \cdot \vec{r}') dS' \end{aligned} \quad (5.13)$$

where $\vec{E}_n(\vec{r}')$ is the electric harmonic field and $\vec{H}_n(\vec{r}')$ is the corresponding magnetic harmonic field with wave number

$$k_n = \omega_n \sqrt{\mu_0 \epsilon_0} \quad (5.14)$$

Eq. (5.13) is a sum over the reflected fields from each of the N harmonic fields which approximate a chirp. Eq. (5.13) is the basis equation for the final calculation in the next chapter where Kirchhoff's approximation is used.

6 KIRCHHOFF'S APPROXIMATION

In this chapter we proceed along the lines in Section 6.6 p. 530-532 in Kong (1986), however, we do a modification which will be clear below. In the Kirchhoff approximation, the fields at any point on the surface are approximated by fields that would be present on the tangent plane at that point (Kong (1986), p. 528). We form an orthonormal system

$$\hat{q}_i = \frac{\hat{k}_i \times \hat{n}}{\left| \hat{k}_i \times \hat{n} \right|} \quad (6.1)$$

which is the local perpendicular polarization vector and \hat{k}_i is the direction of propagation. The local parallel polarization vector is defined by

$$\hat{p}_i = \hat{q}_i \times \hat{k}_i \quad (6.2)$$

The incident electric field is given by

$$\vec{E}_i = \hat{e}_i E_0 \exp(j\vec{k}_{n,i} \cdot \vec{r}) \quad (6.3)$$

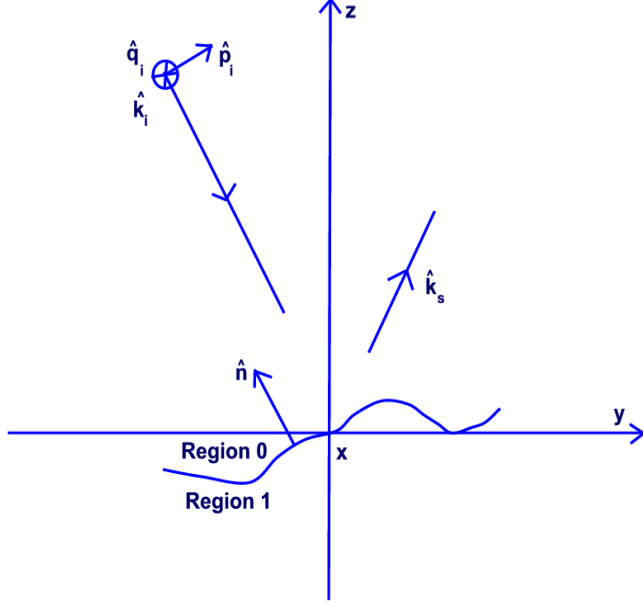


Figure 6.1 Scattering by a random rough surface. Definition of perpendicular (\hat{q}_i) and parallel (\hat{p}_i) polarization of incident field.

where \hat{e}_i is the unit polarization vector. The perpendicular (also called the TE (transverse electric)) component of the incident field is

$$(\hat{e}_i \cdot \hat{q}_i) \hat{q}_i E_0 \exp(j\vec{k}_{n,i} \cdot \vec{r}') \quad (6.4)$$

The local reflected TE component is

$$R_{n,\perp} (\hat{e}_i \cdot \hat{q}_i) \hat{q}_i E_0 \exp(j\vec{k}_{n,r} \cdot \vec{r}') \quad (6.5)$$

where the local reflected direction (specular reflection) is related to the incident direction by

$$\hat{k}_{n,r} = \hat{k}_{n,i} - 2\hat{n}(\hat{n} \cdot \hat{k}_{n,i}) \quad (6.6)$$

and the Fresnel coefficient for the TE component is

$$R_{n,\perp} = \frac{k_n \cos(\theta_i) - \sqrt{k_{n,1}^2 - k_n^2 \sin^2 \theta_i}}{k_n \cos(\theta_i) + \sqrt{k_{n,1}^2 - k_n^2 \sin^2 \theta_i}} \quad (6.7)$$

where

$$k_n = \omega_n \sqrt{\mu_0 \varepsilon_0} \quad (6.8)$$

and

$$k_{n,1} = \omega_n \sqrt{\mu_1 \varepsilon_1} \quad (6.9)$$

μ_0 and ε_0 are the permeability and permittivity in region 0 and μ_1 and ε_1 are the permeability and permittivity in region 1. The total electric field of the TE (perpendicular) component on the boundary is the sum of Eqs. (6.4) and (6.5). The tangential field is the cross product of the surface normal vector, \hat{n} , and the total TE electric field, $\vec{E}_{n,\perp}$

$$\left(\vec{n} \times \vec{E}_{n,\perp} \right) = \left(\hat{n} \times \hat{q}_i \right) \left(\hat{e}_i \cdot \hat{q}_i \right) E_0 \left[\exp\left(j\vec{k}_{n,i} \cdot \vec{r}' \right) + R_{n,\perp} \exp\left(j\vec{k}_{n,r} \cdot \vec{r}' \right) \right] \quad (6.10)$$

The magnetic field associated with the incident electric field in Eq. (6.4) is

$$\frac{E_0}{\eta} \left(\hat{e}_i \cdot \hat{q}_i \right) \left(\hat{k}_i \times \hat{q}_i \right) E_0 \exp\left(j\vec{k}_{n,i} \cdot \vec{r}' \right) \quad (6.11)$$

The magnetic field associated with the reflected field in Eq. (6.5) is

$$\frac{R_{n,\perp} E_0}{\eta} \left(\hat{e}_i \cdot \hat{q}_i \right) \left(\hat{k}_r \times \hat{q}_i \right) E_0 \exp\left(j\vec{k}_{n,r} \cdot \vec{r}' \right) \quad (6.12)$$

Then the total TE (perpendicular) component of the magnetic field is

$$\left(\hat{n} \times \vec{H}_{n,\perp} \right) = \frac{E_0}{\eta} \left(\hat{e}_i \cdot \hat{q}_i \right) \left[\hat{n} \times \left(\hat{k}_i \times \hat{q}_i \right) \exp\left(j\vec{k}_{n,i} \cdot \vec{r}' \right) + \hat{n} \times \left(\hat{k}_r \times \hat{q}_i \right) R_{n,\perp} \exp\left(j\vec{k}_{n,r} \cdot \vec{r}' \right) \right] \quad (6.13)$$

Since we have the following relations

$$\begin{aligned} \hat{n} \times \left(\hat{k}_r \times \hat{q}_i \right) &= \hat{k}_r \left(\hat{n} \cdot \hat{q}_i \right) - \hat{q}_i \left(\hat{n} \cdot \hat{k}_r \right) = \\ &= -\hat{q}_i \cdot \left(\hat{n} \cdot \left(\hat{k}_i - 2\left(\hat{n} \cdot \hat{k}_i \right) \cdot \hat{n} \right) \right) = \left(\hat{n} \cdot \hat{k}_i \right) \hat{q}_i \end{aligned} \quad (6.14)$$

where we have used the rule

$$\vec{a} \times \left(\vec{b} \times \vec{c} \right) = \vec{b} \left(\vec{a} \cdot \vec{c} \right) - \vec{c} \left(\vec{a} \cdot \vec{b} \right) \quad (6.15)$$

and the fact that

$$\hat{n} \cdot \hat{q}_i = 0 \quad (6.16)$$

we get from Eq. (5.13) the total tangential TE component of the magnetic field

$$\begin{aligned} (\hat{n} \times \vec{H}_{n,\perp}) &= \frac{E_0}{\eta} (\hat{e}_i \cdot \hat{q}_i) \\ &\left[-(\hat{n} \times \hat{p}_i) \exp(j\vec{k}_{n,i} \cdot \vec{r}') + (\hat{n} \cdot \hat{k}_i) \hat{q}_i R_{n,\perp} \exp(j\vec{k}_{n,r} \cdot \vec{r}') \right] \end{aligned} \quad (6.17)$$

The TM (parallel) component of the incident electric field is

$$E_0 (\hat{e}_i \cdot \hat{p}_i) \hat{p}_i \exp(j\vec{k}_{n,i} \cdot \vec{r}') \quad (6.18)$$

The TM component of the local reflected electric field is

$$R_{n,\parallel} E_0 (\hat{e}_i \cdot \hat{p}_i) \hat{p}_r \exp(j\vec{k}_{n,r} \cdot \vec{r}') \quad (6.19)$$

where the Fresnel coefficient of the TM (parallel) component is

$$R_{n,\parallel} = \frac{\varepsilon_1 k_n \cos(\theta_i) - \varepsilon_0 \sqrt{k_{n,1}^2 - k_n^2 \sin^2 \theta_i}}{\varepsilon_1 k_n \cos(\theta_i) + \varepsilon_0 \sqrt{k_{n,1}^2 - k_n^2 \sin^2 \theta_i}} \quad (6.20)$$

If we add Eqs. (6.18) and (6.19) we get the TM (parallel) component of total electric field at the reflecting boundary. Using the fact that $\hat{n} \times \hat{p}_r = -\hat{n} \times \hat{p}_i$, the tangential field is

$$(\hat{n} \times \vec{E}_{n,\parallel}) = E_0 (\hat{e}_i \cdot \hat{q}_i) (\hat{n} \times \hat{p}_i) \left[\exp(j\vec{k}_{n,i} \cdot \vec{r}') - R_{n,\parallel} \exp(j\vec{k}_{n,r} \cdot \vec{r}') \right] \quad (6.21)$$

The magnetic fields associated with Eqs. (6.18) and (6.19) are

$$\frac{E_0}{\eta} (\hat{e}_i \cdot \hat{p}_i) (\hat{k}_i \times \hat{p}_i) \exp(j\vec{k}_{n,i} \cdot \vec{r}') \quad (6.22)$$

and

$$\frac{R_{n,\parallel}}{\eta} (\hat{e}_i \cdot \hat{p}_i) (\hat{k}_r \times \hat{p}_r) E_0 \exp(j\vec{k}_{n,r} \cdot \vec{r}') \quad (6.23)$$

The total TM (parallel) component of the magnetic field is the sum of Eqs. (6.22) and (6.23).

Then we get the tangential field

$$(\hat{n} \times \vec{H}_{n,\parallel}) = \frac{E_0}{\eta} (\hat{e}_i \cdot \hat{p}_i) \left[\hat{n} \times (\hat{k}_i \times \hat{p}_i) \exp(j\hat{k}_i \cdot \vec{r}') + R_{n,\parallel} \hat{n} \times (\hat{k}_r \times \hat{p}_r) \exp(j\vec{k}_{n,r} \cdot \vec{r}') \right] \quad (6.24)$$

If we use that $\hat{k}_r \times \hat{p}_r = \hat{k}_i \times \hat{p}_i$ and that $\hat{q}_i = \hat{k}_i \times \hat{p}_i$ we can write Eq. (6.24)

$$(\hat{n} \times \vec{H}_{n,\parallel}) = \frac{E_0}{\eta} (\hat{e}_i \cdot \hat{p}_i) (\hat{n} \times \hat{q}_i) \left[\exp(j\hat{k}_i \cdot \vec{r}') + R_{n,\parallel} \exp(j\vec{k}_{n,r} \cdot \vec{r}') \right] \quad (6.25)$$

The total electric tangential field is given by the sum of Eqs. (6.10) and (6.21)

$$\begin{aligned} (\hat{n} \times \vec{E}_n) = E_0 \left\{ (\hat{e}_i \cdot \hat{q}_i) (\hat{n} \times \hat{q}_i) \left[\exp(j\vec{k}_{n,i} \cdot \vec{r}') + R_{n,\perp} \exp(j\vec{k}_{n,r} \cdot \vec{r}') \right] \right. \\ \left. + (\hat{e}_i \cdot \hat{p}_i) (\hat{n} \times \hat{p}_i) \left[\exp(j\vec{k}_{n,i} \cdot \vec{r}') - R_{n,\parallel} \exp(j\vec{k}_{n,r} \cdot \vec{r}') \right] \right\} \end{aligned} \quad (6.26)$$

The total magnetic field is given by the sum of Eq. (6.17) and (6.25)

$$\begin{aligned} (\hat{n} \times \vec{H}_n) = \frac{E_0}{\eta} \left\{ (\hat{e}_i \cdot \hat{q}_i) \left[-(\hat{n} \times \hat{p}_i) \exp(j\vec{k}_{n,i} \cdot \vec{r}') + (\hat{n} \cdot \hat{k}_i) \hat{q}_i R_{n,\perp} \exp(j\vec{k}_{n,r} \cdot \vec{r}') \right] + (\hat{e}_i \cdot \hat{p}_i) \cdot \right. \\ \left. (\hat{n} \times \hat{q}_i) \left[\exp(j\vec{k}_{n,i} \cdot \vec{r}') + R_{n,\parallel} \hat{n} \times (\hat{k}_r \times \hat{p}_i) \exp(j\vec{k}_{n,r} \cdot \vec{r}') \right] \right\} \end{aligned} \quad (6.27)$$

We note that that if we insert Eqs. (6.26) and (6.27) into Eq. (5.13) we get the scattered field in terms of the geometry and Fresnel coefficients. If we insert Eq. (6.6) into Eq. (6.26) and take the cross product of \hat{k}_s with Eq. (6.26) we get

$$\begin{aligned} \hat{k}_s \times (\hat{n} \times \vec{E}_n) = E_0 \exp(j\vec{k}_{n,i} \cdot \vec{r}') \left\{ (\hat{e}_i \cdot \hat{q}_i) \cdot (\hat{k}_s \times (\hat{n} \times \hat{q}_i)) \left[1 + R_{n,\perp} \cdot \right. \right. \\ \left. \left. \exp(-j2k_n (\hat{n} \cdot \hat{k}_i) (\hat{n} \cdot \vec{r}')) \right] + (\hat{e}_i \cdot \hat{p}_i) \cdot (\hat{k}_s \times (\hat{n} \times \hat{p}_i)) \left[1 - R_{n,\parallel} \exp(-j2k_n (\hat{n} \cdot \hat{k}_i) (\hat{n} \cdot \vec{r}')) \right] \right\} \end{aligned} \quad (6.28)$$

$$\begin{aligned} \eta (\hat{n} \times \vec{H}_n) = E_0 \exp(j\vec{k}_{n,i} \cdot \vec{r}') \left\{ (\hat{e}_i \cdot \hat{q}_i) \cdot \left[-(\hat{n} \times \hat{p}_i) + (\hat{n} \cdot \hat{k}_i) \hat{q}_i R_{n,\perp} \cdot \right. \right. \\ \left. \left. \exp(-j2k_n (\hat{n} \cdot \hat{k}_i) (\hat{n} \cdot \vec{r}')) \right] + (\hat{e}_i \cdot \hat{p}_i) (\hat{n} \times \hat{q}_i) \left[1 + R_{n,\parallel} \exp(-j2k_n (\hat{n} \cdot \hat{k}_i) (\hat{n} \cdot \vec{r}')) \right] \right\} \end{aligned} \quad (6.29)$$

where $\eta = \sqrt{\mu_0 / \varepsilon_0}$ is the intrinsic impedance in region 0. Then we can put Eqs. (6.28) and (6.29) into Eq. (5.13) and we get the scattered field.

$$\begin{aligned} \vec{E}_s(\vec{r}) = E_0 \sum_{n=1}^N \frac{jk_n \exp(jk_n r)}{4\pi r} \left(\vec{I} - \hat{k}_s \hat{k}_s \right) \\ \iint \left\{ \hat{k}_s \times \left[\vec{n} \times \vec{E}_n(\vec{r}') \right] + \eta \left[\vec{n} \times \vec{H}_n(\vec{r}') \right] \right\} \exp(-j(\vec{k}_{n,s} - \vec{k}_{n,i}) \cdot \vec{r}') dS' \end{aligned} \quad (6.30)$$

We remember that the wave vectors are given by $\vec{k}_{n,s} = k_n \hat{k}_s$ and $\vec{k}_{n,i} = k_n \hat{k}_i$ where $k_n^2 = \omega_n^2 \mu_0 \varepsilon_0$ for region 0. Eqs. (6.28), (6.29) and (6.30) are different from the literature (Kong (1986), Franceschetti (2003)) in two ways. First we use incident and scattered wave vectors $\vec{k}_{n,i}$ and $\vec{k}_{n,s}$ as well as Fresnel coefficients $R_{n,\perp}$ and $R_{n,\parallel}$ for angular frequency ω_n , which means different frequencies within the chirp bandwidth. Second, we use another expression for the local reflected field in the specular direction. The TE component of the incident field is given by Eq. (6.4): $(\hat{e}_i \cdot \hat{q}_i) \hat{q}_i E_0 \exp(j\vec{k}_{n,i} \cdot \vec{r}')$. We use the local reflected TE component given by Eq.

(6.5): $R_{n,\perp}(\hat{e}_i \cdot \hat{q}_i) \hat{q}_i E_0 \exp(j\vec{k}_{n,r} \cdot \vec{r}')$ where the specular direction is given by Eq. (6.6):

$\hat{k}_r = \hat{k}_i - 2\hat{n}(\hat{n} \cdot \hat{k}_i)$. In Kong (1986) a monochromatic incident wave vector is used both in the incident and reflected field, which means $\exp(j\vec{k}_i \cdot \vec{r}')$. It should be mentioned that Eq. (6.30) is valid for single scattering. For double scattering new equations have to be calculated.

7 CALCULATION OF SCATTERING ELEMENTS FOR SPECIFIED GEOMETRY

If we assume that we have a planar surface, S' , the surface normal \hat{n} in Eqs. (6.28), (6.29) and (6.30) is a constant over the surface. Then the integral in Eq. (6.30) must be calculated only with the exponential $\exp(-j(\vec{k}_{n,s} - \vec{k}_{n,i}) \cdot \vec{r}')$ as the integrand. Since the r' dependent parts in Eqs. (6.28) and (6.29) are calculated on a flat surface, the exponentials become a constant

$$\exp(-j2k_n(\hat{n} \cdot \hat{k}_{n,i})\hat{n} \cdot \vec{r}') = \exp(-j2k_n(-\cos\theta) \cdot (0,0,1) \cdot (x,y,0)) = 1 \quad (7.1)$$

If we consider the backscatter direction opposite to incident $\hat{k}_s = -\hat{k}_i$, Eq. (6.30) can be simplified as

$$\vec{E}_s(\vec{r}) = E_0 \sum_{n=1}^N \frac{jk_n \exp(jk_n r)}{4\pi r} (\vec{I} - \hat{k}_i \hat{k}_i) \vec{F}_n(\hat{e}_i) I_{n,S} \quad (7.2)$$

where

$$I_{n,S} = \iint \exp(j2\vec{k}_{n,i} \cdot \vec{r}') dS' \quad (7.3)$$

and

$$\begin{aligned} \vec{F}_n(\hat{e}_i) = & \left\{ (\hat{e}_i \cdot \hat{q}_i) \cdot (\hat{k}_s \times (\hat{n} \times \hat{q}_i)) (1 + R_{n,\perp}) + (\hat{e}_i \cdot \hat{p}_i) \cdot (\hat{k}_s \times (\hat{n} \times \hat{p}_i)) (1 + R_{n,\parallel}) - \right. \\ & \left. (\hat{e}_i \cdot \hat{q}_i) \cdot ((\hat{n} \times \hat{p}_i) - (\hat{n} \cdot \hat{k}_i) \hat{q}_i R_{n,\perp}) + (\hat{e}_i \cdot \hat{p}_i) (\hat{n} \times \hat{q}_i) (1 + R_{n,\parallel}) \right\} \end{aligned} \quad (7.4)$$

$I_{n,S}$ can be a random variable if we define a reflecting rough surface. We define as in Franceschetti (2002) the horizontal polarization states for the incident (ih) and scattered (sh) fields

$$\hat{e}_{ih} = \frac{\hat{k}_i \times \hat{z}}{|\hat{k}_i \times \hat{z}|}, \quad \hat{e}_{sh} = \frac{\hat{k}_s \times \hat{z}}{|\hat{k}_s \times \hat{z}|} \quad (7.5)$$

and for the vertical polarization

$$\hat{e}_{iv} = \hat{e}_{ih} \times \hat{k}_i, \quad \hat{e}_{sv} = \hat{e}_{sh} \times \hat{k}_s \quad (7.6)$$

which is shown in Figure 7.1. The simple flat surface is illustrated in this figure where the z -axis and the surface normal are coincident. We now write Eq. (7.2) in terms of the modified Jones scattering matrix

$$\begin{pmatrix} E_{sh} \\ E_{sv} \end{pmatrix} = \sum_{n=1}^N \frac{jk_n \exp(jk_n r)}{4\pi r} \begin{pmatrix} S_{n,hh} & S_{n,vh} \\ S_{n,hv} & S_{n,vv} \end{pmatrix} \begin{pmatrix} E_{n,0h} \\ E_{n,0v} \end{pmatrix} I_{n,S} \quad (7.7)$$

We show how to calculate the scattering elements for the geometry in Figure 7.1. Let us now define the Cartesian scattering vector

$$\vec{S}_{n,p} = (\vec{I} - \hat{k}_i \hat{k}_i) \vec{F}_n(\hat{e}_{ip}) \quad (7.8)$$

We let $\hat{k}_i = (k_{ix}, k_{iy}, k_{iz})$ and if we write out the components in Eq. (7.8) we get

$$\begin{pmatrix} S_{n,px} \\ S_{n,py} \\ S_{n,pz} \end{pmatrix} = \begin{pmatrix} 1 & 0 & 0 \\ 0 & 1 & 0 \\ 0 & 0 & 1 \end{pmatrix} - \begin{pmatrix} k_{ix}k_{ix} & k_{ix}k_{iy} & k_{ix}k_{iz} \\ k_{iy}k_{ix} & k_{iy}k_{iy} & k_{iy}k_{iz} \\ k_{iz}k_{ix} & k_{iz}k_{iy} & k_{iz}k_{iz} \end{pmatrix} \begin{pmatrix} F_{nx}(\hat{e}_{ip}) \\ F_{ny}(\hat{e}_{ip}) \\ F_{nz}(\hat{e}_{ip}) \end{pmatrix} \quad (7.9)$$

where p is either h or v . Since $k_{ix} = 0$ and $k_{iy} = -\sin\theta$ and $k_{iz} = -\cos\theta$ we get

$$\begin{pmatrix} S_{n,px} \\ S_{n,py} \\ S_{n,pz} \end{pmatrix} = \begin{pmatrix} F_{nx}(\hat{e}_{ip}) \\ \cos^2\theta F_{ny}(\hat{e}_{ip}) - \cos\theta \sin\theta F_{nz}(\hat{e}_{ip}) \\ -\cos\theta \sin\theta F_{ny}(\hat{e}_{ip}) + \sin^2\theta F_{nz}(\hat{e}_{ip}) \end{pmatrix} \quad (7.10)$$

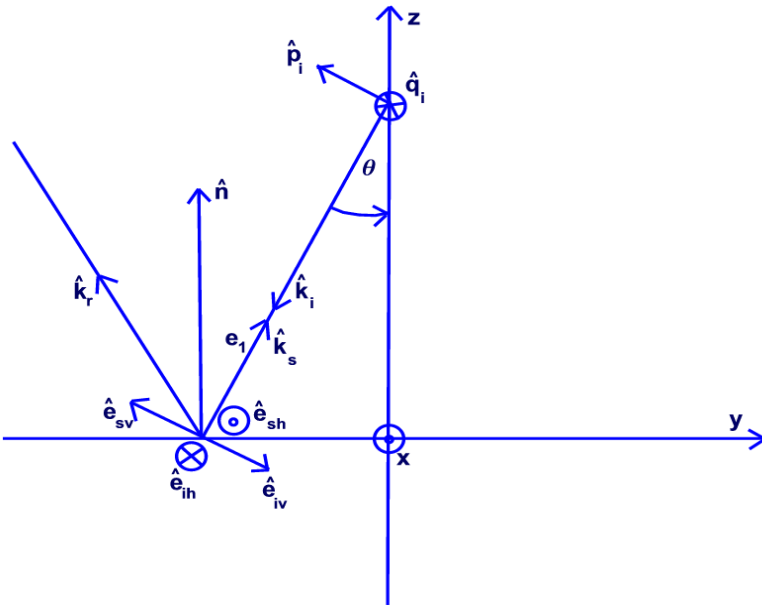


Figure 7.1 Scattering from a plane surface. Definition of horizontal and vertical polarization.

The scattering elements $S_{n,hh}, S_{n,hv}, S_{n,vh}, S_{n,vv}$ can be defined in the following way

$$S_{n,hh} = [S_{n,hx}, S_{n,hy}, S_{n,hz}] \cdot \hat{e}_{sh} \quad (7.11)$$

$$S_{n,hv} = [S_{n,vx}, S_{n,vy}, S_{n,vz}] \cdot \hat{e}_{sh} \quad (7.12)$$

$$S_{n,vh} = [S_{n,hx}, S_{n,hy}, S_{n,hz}] \cdot \hat{e}_{sv} \quad (7.13)$$

$$S_{n,vv} = [S_{n,vx}, S_{n,vy}, S_{n,vz}] \cdot \hat{e}_{sv} \quad (7.14)$$

To calculate the scattering elements we look at Figure 7.1 and calculate the vectors needed to calculate Eqs. (7.4), (7.5), and (7.6)

$$\begin{aligned} \hat{e}_{ih} &= (-1, 0, 0), \quad \hat{e}_{iv} = (0, \cos \theta, -\sin \theta), \quad \hat{e}_{sh} = (1, 0, 0), \quad \hat{e}_{sv} = (0, -\cos \theta, \sin \theta), \quad \hat{q}_i = (-1, 0, 0), \\ \hat{k}_i &= (0, -\sin \theta, -\cos \theta), \quad \hat{p}_i = \hat{q}_i \times \hat{k}_i = (0, -\cos \theta, \sin \theta), \quad \hat{n} = (0, 0, 1), \quad \hat{n} \times \hat{q}_i = (0, -1, 0), \\ \hat{n} \times \hat{p}_i &= (\cos \theta, 0, 0), \quad \hat{k}_s \times (\hat{n} \times \hat{q}_i) = (\cos \theta, 0, 0), \quad \hat{k}_s \times (\hat{n} \times \hat{p}_i) = (0, \cos^2 \theta, -\cos \theta \sin \theta), \\ \hat{e}_{ih} \cdot \hat{q}_i &= (-1, 0, 0) \cdot (-1, 0, 0) = 1, \quad \hat{e}_{iv} \cdot \hat{q}_i = 0, \quad \hat{e}_{ih} \cdot \hat{p}_i = 0, \quad \hat{e}_{iv} \cdot \hat{p}_i = -1, \quad \hat{n} \cdot \hat{k} = -\cos \theta \end{aligned}$$

Using these vectors in Eq. (7.8) we get

$$\vec{F}_n(\hat{e}_{ih}) = (2 \cos \theta (1 + R_{n,\perp}), 0, 0) \quad (7.15)$$

Calculation of Eq. (7.10) yields

$$\vec{S}_{n,p} = \begin{pmatrix} S_{n,px} \\ S_{n,py} \\ S_{n,pz} \end{pmatrix} = \begin{pmatrix} F_{nx}(\hat{e}_{ih}) \\ \cos^2 \theta F_{ny}(\hat{e}_{ih}) - \cos \theta \sin \theta F_{nz}(\hat{e}_{ih}) \\ -\cos \theta \sin \theta F_{ny}(\hat{e}_{ih}) + \sin^2 \theta F_{nz}(\hat{e}_{ih}) \end{pmatrix} = \begin{pmatrix} 2 \cos(\theta) R_{n,\perp} \\ 0 \\ 0 \end{pmatrix} \quad (7.16)$$

Finally we calculate the scattering elements in Eqs. (7.11)-(7.14)

$$S_{n,hh} = [S_{n,hx}, S_{n,hy}, S_{n,hz}] \cdot \hat{e}_{sh} = 2 \cos \theta (R_{n,\perp}) \quad (7.17)$$

$$S_{hh} = 2 \cos(\theta) R_{\perp} \quad (7.18)$$

$$\begin{pmatrix} S_{n,hh} & S_{n,vh} \\ S_{n,hv} & S_{n,vv} \end{pmatrix} = \begin{pmatrix} 2 \cos \theta (R_{n,\perp}) & 0 \\ 0 & -2 \cos \theta (R_{n,\parallel}) \end{pmatrix} \quad (7.19)$$

For the harmonic wave (if we omit the index n) this is equivalent to the result in Franceschetti (2002).

8 INVERSE-EETF FOR RAW DATA SIMULATION

The EETF (Extended Exact Transfer Function) is an algorithm which was developed optimized for spaceborne SAR processing. It is shown in Eldhuset (2004) that the spaceborne formalism which the EETF4 (4th order) is based upon is necessary in order to represent the azimuth phase history with sufficient accuracy for high squint and spatial resolution less than 1 m for X-band. A spotlight raw data simulator for extended scenes was for the first time published in Cimmino (2003) where the focus depth variation is taken care of for a non-squinted geometry and a straight line flight path. The Inverse-EETF4 used in Eldhuset (2004) is a unique raw data simulator for extended scenes with very high resolution. The space-variance of the SAR transfer function is handled in the same way as in the EETF4 for squinted SAR and a very long synthetic aperture of a curved orbit. The Inverse-EETF4 simulates raw data for extended targets for a squinted SAR in a very efficient way by using multi-block processing and handles the enormous range migration in a very compact way, as shown in Figure 8.1. In the left figure the raw data of a point target P is continuous. In the right figure the same raw data are split into two parts P_1 and P_2 where the matrix is half of the size in range. If there is very large range cell migration the point target may be split into n partial point targets (P_1, \dots, P_n). The clue is that there must be enough space in the matrix in the frequency domain. It is concluded in Eldhuset (2004) that the EETF4 algorithm is a good candidate for future ultra high resolution (0.3 m) spaceborne SAR processing. Its novel properties are also mentioned in Fornaro et al (2002) and in Wang and Liu (2004).

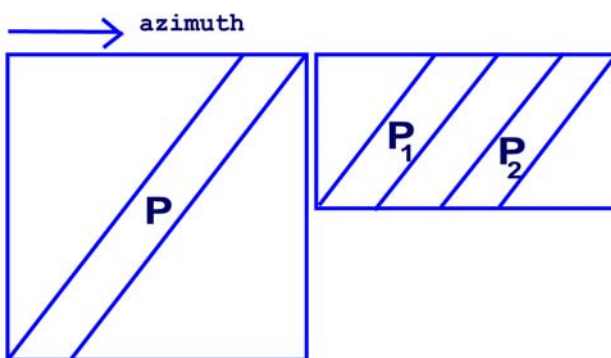


Figure 8.1 Continuous raw data (P) and discontinuous raw data (P_1, P_2) of a point target. (Time domain in both azimuth and range).

The exact transfer function up to fourth order (ETF4) can be found in Eldhuset (1998) and is given by

$$H_{ETF4}(\omega_r, \omega_a; R) = \mathbb{C}_a F_r \left\{ \exp[j\Phi_r(t_r)] \right\} \exp[j\phi(t_a^*)] \quad (8.1)$$

where $F_r \left\{ \exp[j\Phi_r(t_r)] \right\}$ is the Fourier transform of the range chirp and the phase function $\phi(t_a^*)$ is given by

$$\phi(t_a^*) = \lambda \left(a_1 t_a^* + \frac{a_2}{2} (t_a^*)^2 + \frac{a_3}{3} (t_a^*)^3 + \frac{a_4}{4} (t_a^*)^4 \right) \cdot \left(\frac{2\pi}{\lambda} + \frac{\omega_r}{c} \right) - \omega_a t_a^* \quad (8.2)$$

and t_a^* is the stationary point of the equation

$$\left(2\pi + \frac{\lambda\omega_a}{c} \right) \left(a_1 + a_2(t_a) + a_3(t_a)^2 + a_4(t_a)^3 \right) = 0 \quad (8.3)$$

The Doppler parameters are denoted $a_1, a_2, a_3, a_4, \omega_r$ and ω_a are the range and azimuth angular frequencies. The ETF4 is multiplied by the data before the inverse 2 D FFT in Figure 8.2. The phase correction $\Delta\phi_{ETF4}(\omega_a; R, R_m)$ is applied after the azimuth FFT in every azimuth line (at range R_m) and the expressions for $\Delta\phi_{ETF4}(\omega_a; R, R_m)$ can be found in Eldhuset (1998) or compactly written as in Eldhuset (2004)

$$\nabla\phi_{ETF4}(\omega_a; R, R_m) = \nabla\phi_{ETF4} \left[\omega_a; a_1(R_m), a_2(R_m), a_3(R_m), a_4(R_m); a_1(R), a_2(R), a_3(R), a_4(R) \right] \quad (8.4)$$

R is the slant range for a given azimuth line in a block and R_m is the slant range in the middle Figure 8.3. Here the raw data output in Figure 8.2 have been processed with the EETF4 algorithm. Point targets with strong values in single points have been put into $\sigma(t_r, t_a)$. In the future we will implement the calculation of the reflectivity matrix $\sigma(t_r, t_a)$ in terms of Eq. (6.30).

It is mentioned in Touzi and Raney (2004) that the four elements $S_{hh}, S_{hv}, S_{vh}, S_{vv}$ of the scattering matrix will be affected if the Doppler parameters a_1 and a_2 are erroneous. This means that the scattering elements for moving targets will be affected if they have not been re-focused. The effect on the scattering elements could be studied with a total polarimetric modelling also including SAR processing. Another novel application of the Inverse-EETF2 or the Inverse-EETF4 is the simulation of two raw data sets from each of the sub-apertures of the antenna of an along-track MTI (Moving Target Indicator). Clutter, thermal noise and noise due to decorrelations between the channels or moving extended targets or point targets can be simulated. The additional phase of the moving targets can be superposed on the matrix $\sigma(t_r, t_a)$ in one of the raw data sets.

The scattered field in Eq. (6.30) was calculated under the assumption that the surface was smooth. If we assume that the surface is rough and described in a statistical manner, it is

possible to calculate expressions for the mean scattered field of Eq. (6.30) and its standard deviation. The surface can for example be specified by a Gaussian height distribution.

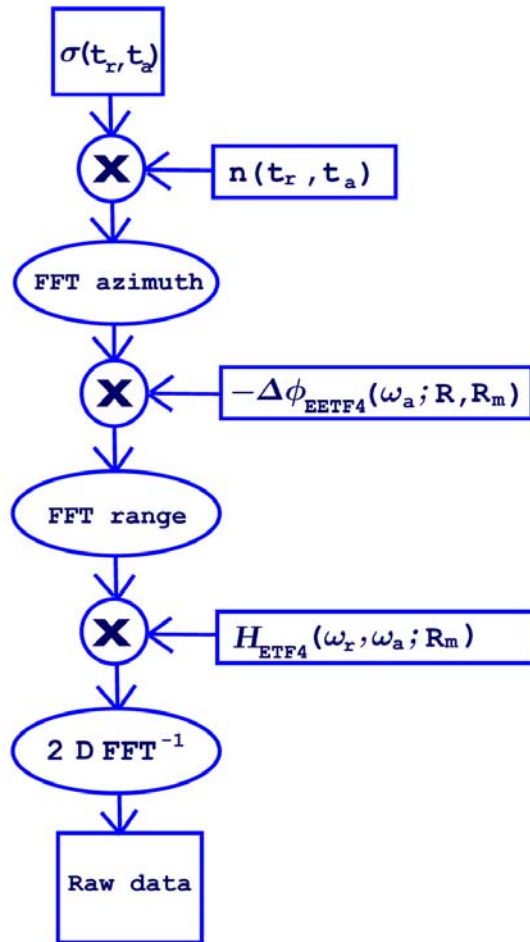


Figure 8.2 The Inverse-EETF4 algorithm where many blocks of raw data in range can be processed.

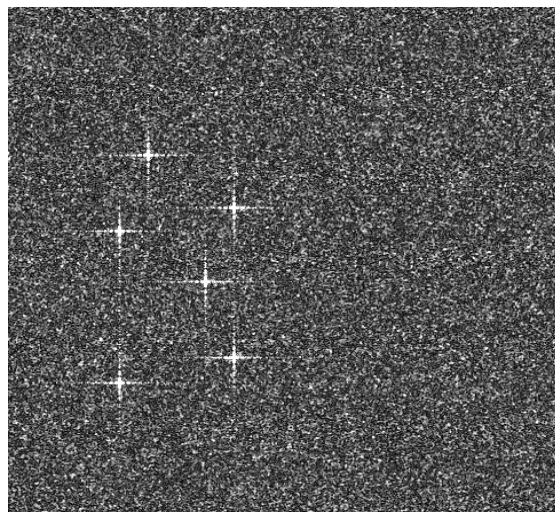


Figure 8.3 Simulation of point targets in clutter using the Inverse-EETF4 followed by EETF4.

9 CONCLUSION

A method for calculation of the reflectivity matrix for spaceborne polarimetric SAR has been outlined. The existing scattering theory has been briefly reviewed and revised for very high resolution. It is shown how the reflectivity matrix can be used as input to the Inverse-EETF4 raw data generator. The single scattering case has been considered. More calculations must be done for double scattering and for rough surfaces. The deterioration of polarimetric characterization of moving targets can be studied by a total modelling of both scattering and SAR processing.

REFERENCES

- Cimmino, S., Franceschetti, G., Iodice, A., Riccio, D., Ruello, G., Efficient spotlight SAR Raw signal simulation of extended scenes. *IEEE Transactions on Geoscience and Remote Sensing*, **41**, 10 (Oct. 2003), 2329-2337.
- Eldhuset, K., A new fourth-order processing algorithm for spaceborne SAR. *IEEE Transactions on Aerospace and Electronic Systems*, **34**, 3 (July 1998), 824-835.
- Eldhuset, K., Ultra high resolution spaceborne SAR processing. *IEEE Transactions on Aerospace and Electronic Systems*, **40**, 1 (Jan. 2004), 370-378.
- Fornaro, G., Sanosti, E., Lanari, R., Tesauro, M., Role of Processing Geometry in SAR Raw Data Focusing. *IEEE Transactions on Aerospace and Electronic Systems*, **38**, 2 (April 2002), 441-453.
- Franceschetti, G., Iodice, A., Riccio, D., A canonical problem in electromagnetic backscattering from buildings. *IEEE Transactions on Geoscience and Remote Sensing*, **40**, 8 (Aug. 2002), 1787-1801.
- Kong, J.A., *Electromagnetic wave theory*. New York, NY:John Wiley & Sons, Inc., 1986.
- Paul, C.R., Nasar S.A., *Electromagnetic fields*. New York:McGraw-Hill, 1987.
- Touzi, R., Raney, K., On the Use of Permanent Symmetric Scatterers for Ship Characterization. *IEEE Transactions on Geoscience and Remote Sensing*, **42**, 10 (Oct. 2004), 2039-2045.
- Wang, K., Liu, X., Squint-Spotlight SAR Imaging by Sub-band Combination and Range-Walk Removal, In *Proceedings of IGARSS'2004*, Anchorage, Sept. 20-24, 2004.